Experimental and Molecular Pathology 109 (2019) 51–60

Contents lists available at ScienceDirect

Experimental and Molecular Pathology

journal homepage: www.elsevier.com/locate/yexmp

Catalpol inhibits cell proliferation, invasion and migration through regulating miR-22-3p/MTA3 signalling in hepatocellular carcinoma

Lina Zhao[a,b], Yishuo Wang[b,*], Qinrong Liu[b]

[a] School of Chinese Medicine, Zhengzhou Railway Vocational and Technical College, Zhengzhou City, Henan Province, China
[b] Department of Science and Technology, Henan University of Chinese Medicine, Zhengzhou City, Henan Province, China

ARTICLE INFO

Keywords:
Hepatocellular carcinoma
Catalpol
miR-22-3p
MTA3
Invasion
Migration

ABSTRACT

Hepatocellular carcinoma (HCC) is the most common type of liver malignancy with high rates of recurrence and mortality worldwide. Unfortunately, effective strategies for the management of HCC are still unsatisfactory. The aim of this investigation is to explore the effects of catalpol on HCC progression and investigated the mechanistic functions of catalpol in HCC. Catalpol significantly suppressed cell viability, caused the suppression in colony growth, decreased number of invaded and migrated HCC cells, and increased the rates of apoptotic cells and proportions of HCC cells at G_0/G_1 cell cycle phase. Furthermore, catalpol dramatically up-regulated miR-22-3p expression in HCC cells, and knockdown of miR-22-3p attenuated the anti-tumor effects of catalpol in HCC. Additionally, results from luciferase reporter assay demonstrated that miR-22-3p targeted the metastasis associated 1 family member 3 (MTA3) 3′untranslated region (3′UTR), and miR-22-3p down-regulated MTA3 expression in HCC cells. Overexpression of MTA3 enhanced HCC cell proliferative abilities, increased the number of invasive and migratory HCC cells, and also attenuated the anti-tumor potentials of catalpol in HCC. Catalpol suppressed HCC tumor growth and increased miR-22-3p expression, while down-regulated MTA3 expression in dissected tumor tissues from xenograft nude mice. Collectively, our results for the first time revealed the anti-tumor potentials of catalpol in HCC, and the anti-tumor effects mediated by catalpol were via modulating the miR-22-3p/MTA3 axis in HCC.

1. Introduction

Hepatocellular carcinoma (HCC) has high rates of recurrence and mortality and is the most common type of liver malignancy worldwide (Khemlina et al., 2017). HCC caused > 0.6 million death annually with the highest rates of death in eastern and south-eastern Asia (Clark et al., 2015). Multiple factors including alcohol consumption, hepatic toxins, infections with hepatitis viruses, genetic modification are found to be important contributors for the pathogenesis of HCC (Forner et al., 2012). Early stage HCC can be treated by curative surgery or liver transplantation (Ozer Etik et al., 2017), however, for the advanced stage HCC, the therapeutic strategies are far from satisfactory due to the tumor recurrence and disease relapse after therapy as well as drug resistance (Grandhi et al., 2016). In this regard, it is urgent for the scientists to find novel compounds with anti-tumor activities for the development of better therapies for HCC.

Catalpol can be extracted from the fresh root of *Rehmannia glutinosa* and is a type of iridoid glycoside compound (Wang and Zhan-Sheng, 2018). The pharmacological activities of catalpol including anti-tumor, anti-inflammatory actions as well as hypoglycaemic activities were identified by previous studies (Li et al., 2014; Zheng et al., 2017). The anti-tumor potentials of catalpol have been demonstrated in various tumor malignancies including colon cancer, breast cancer, gastric cancer, osteosarcoma, ovarian cancer, lung cancer and bladder cancer, and various molecular mechanisms underlying the anti-tumor effects of catalpol have been proposed (Gao et al., 2014; Jin et al., 2015; Liu et al., 2015; Liu et al., 2017; Wang and Xue, 2018; Wang et al., 2018b; Wang and Zhan-Sheng, 2018; Zhu et al., 2017). However, as far as we know, the anti-tumor potentials of catalpol in HCC have not been investigated yet.

MicroRNAs (miRNAs) belong to a type of short non-coding RNAs with ~22 nucleotides, and miRNAs exerted its functions via targeting the 3′ untranslated region (3′UTR) of the genes, which subsequently causes repression of targeted genes (Xu et al., 2018). MiRNAs are found to involve in diverse biological processes particularly in the cancer progression. A large number of miRNAs such as miR-22-3p, let-7a, miR-26a, miR-125b, miR-155, miR-10a, miR-221 and miR-224 has be identified for their essential roles in the regulation of HCC progression

* Corresponding author at: Department of Science and Technology, Henan University of Chinese Medicine, Zhengzhou City, Henan Province, 451460, China.
E-mail address: 895027475@qq.com (Y. Wang).

https://doi.org/10.1016/j.yexmp.2019.104265
Received 17 February 2019; Received in revised form 13 April 2019; Accepted 24 May 2019
Available online 27 May 2019
0014-4800/

(Morishita and Masaki, 2015).

In our experiments, we evaluated the anti-tumor potentials of catalpol in the HCC cell lines, and further explored the molecular mechanisms underlying catalpol-mediated anti-tumor effects in HCC. Our results identified miR-22-3p/metastasis associated 1 family member 3 (MTA3) axis as one of the important signalling pathways in mediating the anti-tumor potentials of catalpol in HCC. Our investigations may provide novel understandings about the anti-tumor actions of catalpol in HCC.

2. Materials and methods

2.1. Cell lines and cell culture

HCC cell lines including Huh7 and HCCLM3 cells (Cell Bank of Chinese Academy Sciences, Shanghai, China) were kept in the Dulbecco's Modified Eagle's Medium (DMEM; Sigma, St. Louis, USA) with 10% fetal bovine serum (FBS; Gibco, Carlsbad, USA). The Huh7 and HCCLM3 cells kept in a humidified cell culture incubator supplying with 5% CO_2 gas at 37 °C.

2.2. MiRNAs, vectors, cell transfections and catalpol treatments

The miRNA mimics for miR-22-3p, the negative control (NC) for miR-22-3p mimics, the inhibitors for miR-22-3p (anti-miR-22-3p) and the inhibitors NC (anti-miR NC) were obtained from Ribobio (Guangzhou, China). The control pcDNA3.1 vector as well as the MTA3-overexpressing vectors (pcDNA3.1-MTA3) were constructed by GenePharma (Shanghai, China). HCC cell transfections for miRNAs and vectors were carried using the Lipofectamine 2000 reagent complying with manufacturer's manual (Invitrogen, Carlsbad, USA). For the catalpol (Sigma, St. Louis, USA) treatments, HCC cells were treated by increased concentrations (2.5, 5, 10, 20, 50 and 100 μM) of catalpol for 24, 48 and 72 h, respectively.

2.3. Isolation of RNA and gene expression as determined by quantitative real-time PCR (qRT-PCR)

Total RNA isolation from HCC cells and dissected tumors was carried out using TRIzol reagent (Invitrogen). cDNA was obtained from reversely transcribed RNA by using the M-MLV reverse transcriptase (Invitrogen). Applied Biosystems 7900 Real-time PCR system (Applied Biosystems, Foster City, USA) was used perform the real-time PCR reactions by using SYBR Premix EX Taq™ II kit (Takara, Dalian, China) in an. The relative expressions of miRNAs and MTA3 mRNA were calculated by following the comparative threshold temperature method. U6 and glyceraldehyde 3-phosphate dehydrogenase were served as internal controls for miRNAs and MTA3, respectively. The primers were provided in Supplemental Table S1.

2.4. Western blot

Proteins isolation from cells were performed using RIPA lysis buffer (Sigma). The extracted proteins were separated by the 10% sodium dodecyl sulfate polyacrylamide gel electrophoresis, and then the proteins were transferred to a polyvinylidene fluoride (PVDF) membrane. The PVDF membrane was then incubated with 5% non-fat milk in phosphate buffered saline with Tween 20 (PBST) at room temperature for 1 h before the membranes being incubated with antibodies for MTA3 (Cell Signalling Technology, Danvers, USA) and β-actin (Cell Signalling Technology) overnight at 4 °C. Then the PVDF membrane were washed with PBST for 3 times followed by incubating the corresponding secondary antibodies with horseradish peroxidase-conjugation at room temperature for the duration of 2 h, and the enhanced chemiluminescence substrate kit was used to detect the bands (Bio-Rad, Hercules, USA).

2.5. Cell viability as detected by MTT assay

The cell viability of Huh7 and HCCLM3 cells were evaluated by the MTT assay. Briefly, the treated cells (Huh7 and HCCLM3 cells) were treated with 5 mg/ml MTT (20 μl) at 37 °C for a duration of 4 h followed by dissolving the formazan with100 μl of dimethyl sulfoxide. The cell viability was assessed by measuring the optical density values at 570 nm wavelength with a microplate reader.

2.6. Cell growth as detected by colony formation assay

The cell growth of Huh7 and HCCLM3 cells was assessed by colony formation assay. Briefly, the treated Huh7 and HCCLM3 cells were seed onto the petri dish at a 300 cells/dish with 2 ml of culture media, and the Huh7 and HCCLM3 cells were further cultured at 37 °C with 5% CO_2 for 2 weeks. The fixation of colonies was performed by incubating with paraformaldehyde (4% in phosphate buffered saline) for a duration of 15 min followed by staining with 0.1% gentian violet at room temperature for a duration of 10 min, and the number of the stained colonies was determined under a microscope.

2.7. Cell invasion and migration as detectedTranswell invasion and migration assays

Cell invasive and migratory abilities of Huh7 and HCCLM3 cells were carried by using the Transwell system (Corning Costar, Lowell, USA). Briefly, treated Huh7 and HCCLM3 cells (treatment with catalpol for 48 h or transfection with different oligonucleotides) were plated on the upper side of the transwell inserts (polycarbonate membrane in 8 μm pore size) with Matrigel-coated (for invasion assays) or without Matrigel (for migration assays) in the top chamber, and the top chamber was added with DMEM without FBS, while DMEM medium supplied with 10% FBS was filled into the bottom chamber. The Huh7 and HCCLM3 cells were incubated in the upper chamber for 24 h at 37 °C. The clean cotton swabs were used to wipe the non-invasive or non-migrated cells from the top chamber, and the fixation of invaded and migrated cells on the bottom chamber surface were performed by incubating with paraformaldehyde (4% in phosphate buffered saline) for a duration of 15 min followed by staining with 0.1% gentian violet at room temperature for a duration of 10 min. The number of invaded and migrated cells were evaluated using a light microscope in five randomly selected fields.

2.8. Flow cytometry to determine cell apoptosis and cell cycle

The cell apoptotic rates of Huh7 and HCCLM3 cells were determined by using Cell Apoptosis Detection Kit (BD Biosciences, Franklin Lakes, USA). Briefly, the treated cells (Huh7 and HCCLM3 cells) were collected and washed twice with phosphate buffered saline followed by re-suspending in binding buffer. After that, the cells were incubated with Annexin V-FITC and propidium iodide solutions at room temperature for a duration of 15 min in the dark, and apoptotic rates of Huh7 and HCCLM3 cells were determined on a FACS Calibur system (BD Biosciences).

For the determination of cell cycle, treated Huh7 and HCCLM3 cells were trypsinized and washed with ice-cold phosphate buffered saline twice and then Huh7 and HCCLM3 cells were further incubated with cell cycle staining buffer containing propidium iodide (BD Biosciences) at room temperature for a duration of 30 min. After that, cells were sorted and evaluated on a FACS Calibur flow cytometer (BD Biosciences).

2.9. Luciferase reporter assay

We constructed luciferase reporter vectors by inserting MTA3 3′UTR segments (wild type or mutant) into the pmirGLO reporter plasmids

(Promega, Madison, USA). For the luciferase reporter activity determination, HCCLM3 cells were co-transfected with miRNAs (mimics NC or miR-22-3p mimics) and luciferase reporter vectors (containing wild type MTA3 3′UTR or MTA 3′UTR with point mutations). Forty-eighth later, Dual-Luciferase reporter system (Promega) was employed to measure the relative luciferase activity by following the manufacturer's instructions.

2.10. In vivo nude mice model for HCC tumor growth

The 5-week-old male nude mice were obtained from Henan Laboratory Animal Center (Zhengzhou, China). All the animal experimental procedures were under the approval from the Ethics Committee for Animal Experiments of Henan University of Chinese medicine. Briefly, 1×10^6 HCCLM3 cells were administered subcutaneously into the dorsal flanks of the mice. The tumor-bearing nude mice were randomly orally administered with vehicle or different doses (10 mg/kg, 20 mg/kg or 50 mg/kg) of catalpol every day for 30 days, and determination of tumor volume was carried out every 5 days. The tumor volume was determined by the following formula: $0.5 \times (L \times L \times H$; L: the long diameter; H: the height of the tumor). At 30 days after tumor cells inoculation, overdose of pentobarbitone was used to sacrifice the mice, and tumor tissues were weighed and collected for qRT-PCR analysis.

2.11. Statistical analysis

GraphPad Prism 7.0 version (GraphPad Software, La Jolla, USA) was used to do graph plotting and statistical analysis. Data were presented as mean ± standard deviation. The data were analysed using one-way analysis of variance with Turkey's post-hoc tests or unpaired Student's *t*-test based on group number. A P value of < 0.05 was defined as statistically significant.

3. Results

3.1. Catalpol suppressed cell viability in HCC cells in concentration- and time-dependent manners

To determine anti-tumor potentials of catalpol in the HCC, we treated the HCC cell lines (Huh7 and HCCLM3) with increased concentrations of catalpol for different durations, respectively. As shown in Fig. 1A, Huh7 received treatments with catalpol (2.5, 5, 10, 20, 50 and 100 μM) for 24, 48 and 72 h showed marked reduction of cell viability of Huh7 and HCMML2 cells and the effects were concentration- and time-dependent, and catalpol at 50 μM concentration for the above time durations caused > 50% reduction of cell viability of Huh7 cells. Consistently, the inhibitory effect of catalpol on the cell viability of HCCLM3 was concentration- and time-dependent (Fig. 1B). As catalplol at 50 μM treatment for 48 h got > 50% reduction of cell viability in Huh7 and HCCLM3 cells, we selected 50 μM with 48 h treatment for further in vitro functional assays.

3.2. Catalpol inhibited cell proliferative, invasive and migratory abilities of Huh7 and HLCCM2 cells

To illustrate the effects of catalpol on the HCC progression, we determined the effects of catalpol on the cell proliferative, cell invasive and migratory abilities of Huh7 and HCCLM3 cells by using different functional in vitro assays. Fig. 2A and B demonstrated that catalpol (50 μM) for 48 h treatment obviously reduced the colony number in both Huh7 and HCCLM3 cells when compared to vehicle group (Fig. 2A and B). Additionally, Huh7 and HCCLM3 cells received catalpol (50 μM) treatment for 48 h showed a reduced invasive capacity when compared to vehicle group (Fig. 2C and D). Consistently, the transwell migration assay also showed catalpol (50 μM) with treatment duration of 48 h caused a reduction in the migrated Huh7 and HCCLM3 cell number (Fig. 2E and F). Collectively, these data indicated that catalpol had the inhibitory actions on the HCC cell proliferative, invasive and migratory abilities.

3.3. Catalpol increased cell apoptotic rates and cell proportions at G0/G1 phase of Huh7 and HCLMM2 cells

The effects of catalpol on the cell apoptotic rates and cell cycle of HCC cells were further evaluated by the flow cytometry analysis. Fig. 3A and B showed that catalpol (50 μM) treatment for 48 h significantly induced cell apoptosis, where the cell apoptotic rates of Huh7 and HCCLM3 cells increased to > 30% after catalpol treatment. In addition, catalpol (50 μM) treatment for 48 h increased cell number atG_0/G_1 cell cycle and decreased cell number at S cycle cell in both Huh7 and HCCLM3 cells (Fig. 3C and D). Taken together, the flow cytometry results implied that catalpol increased cell apoptotic rates and cell proportions at G0/G1 phase of Huh7 and HCLMM2 cells.

3.4. The inhibitory effects of catalpol-mediated cell proliferative, invasive and migratory abilities of HCC cells were via up-regulating miR-22-3p

As miRNAs have been implicated for their important roles in HCC progression, we determined the actions of catalpol (50 μM) on the expression of the miRNAs including miR-22-3p, let-7a, miR-26a, miR-125b, miR-155, miR-10a, miR-221 and miR-224 in Huh7 and HCCLM3 cells. Catalpol (50 μM) treatment significantly up-regulated the expression levels of miR-22-3p and let-7a, and the expression level of

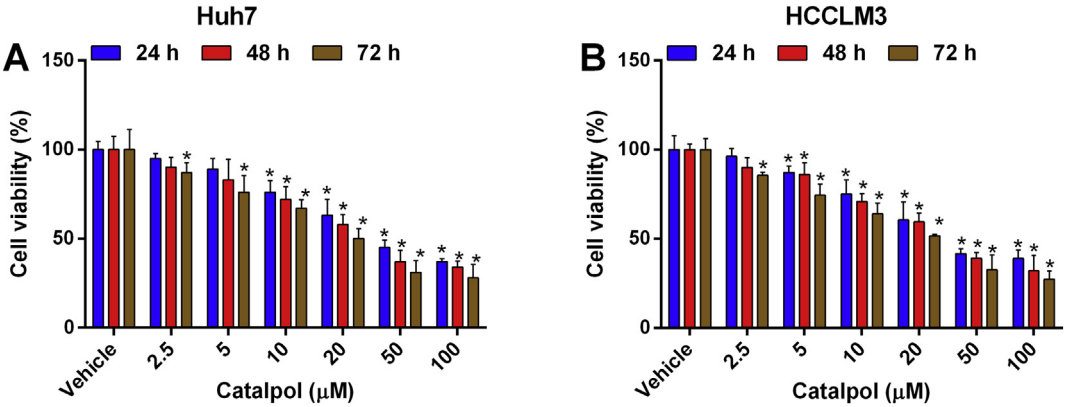

Fig. 1. Catalpol suppressed cell viability in HCC cells. (A) The cell viability of Huh7 cells was examined by MTT assay, cells were treated with different concentrations of catalpol (2.5, 5, 10, 20, 50 and 100 μM) for 24, 48 and 72 h, respectively. (B) The cell viability of HCCLM3 cells was examined by MTT assay, cells were treated with different concentrations of catalpol (2.5, 5, 10, 20, 50 and 100 μM) for 24, 48 and 72 h, respectively. $N = 3$; $^*P < .05$ versus the respective vehicle groups.

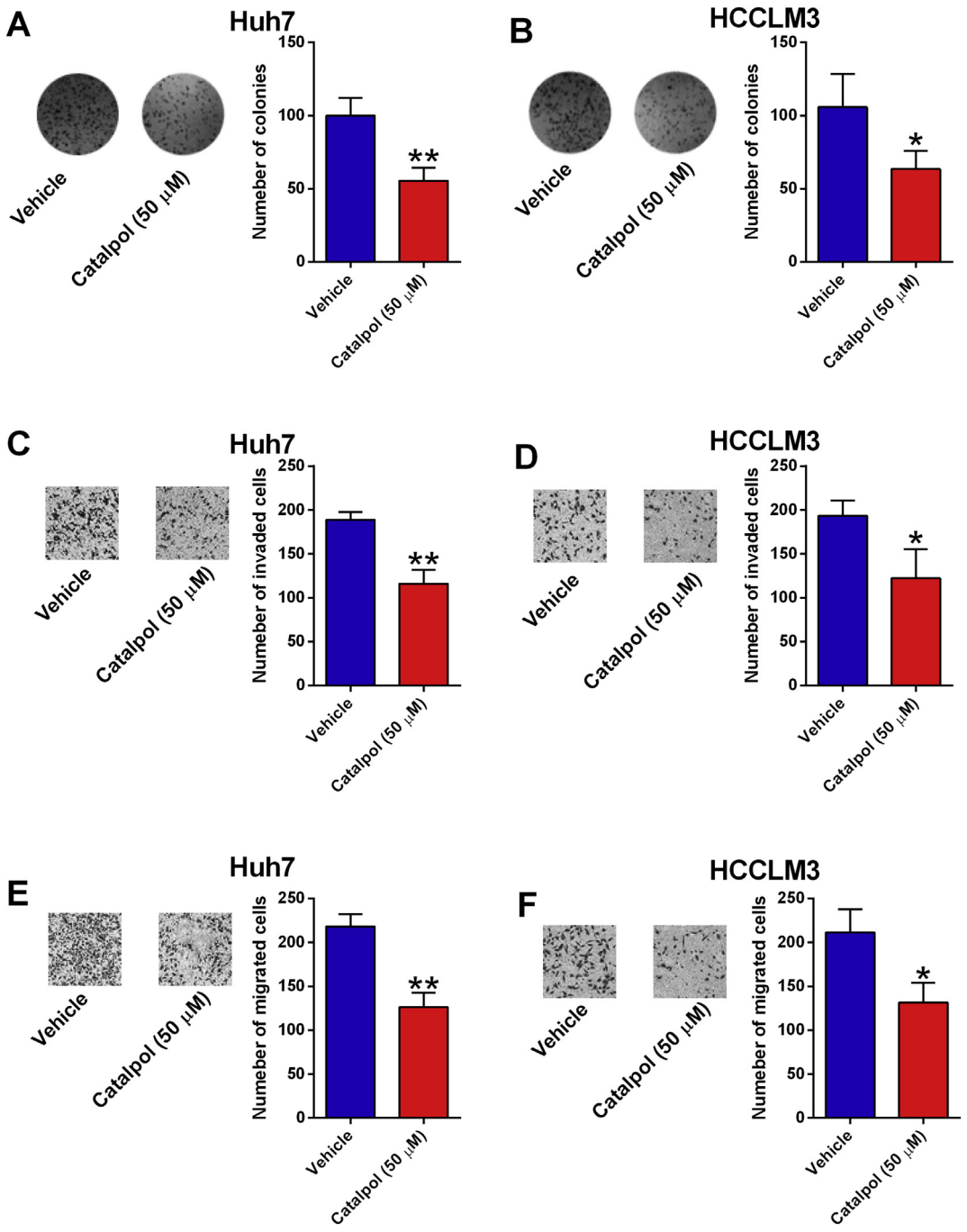

Fig. 2. Catalpol inhibited cell proliferation, invasion and migration of HCC cells. (A and B) The cell proliferation of Huh7 and HCCLM3 was determined by colony formation assay. Cells were treated with vehicle or catalpol (50 μM) for 48 h. (C and D) The cell invasion of Huh7 and HCCLM3 cells was determined by transwell cell invasion assay. Cells were treated with vehicle or catalpol (50 μM) for 48 h. (E and F) The cell migration of Huh7 and HCCLM cells was determined by transwell migration assay. Cells were treated with vehicle or catalpol (50 μM) for 48 h. $N = 3$; $^{*}P < .05$ and $^{**}P < .01$ versus the vehicle group.

miR-22-3p was elevated by around 5 fold after catalpol treatment in Huh7 and HCCLM3 cells; while other miRNAs expression levels were not affected (Fig. 4A and B). Furthermore, we examined if the miR-22-3p mediated the suppressive effects of catalpol on the cell proliferative, invasive and migratory abilities of Huh7 and HCCLM3 cells. Huh7 and HCCLM3 cells were first transfected by anti-miR-22-3p or anti-miR NC, and 24 h post-transfection, the cells were treatment with catalpol (50 μM) for 48 h, and then the cell proliferative, cell invasive and migratory abilities were evaluated by different functional in vitro assays, respectively. Transfection with anti-miR-22-3p significantly suppressed the miR-22-3p expression in Huh7 and HCCLM3 cells when compared to anti-miR NC group (Fig. 4C and D). The functional in vitro assays revealed that inhibition of miR-22-3p by transfecting HCC cells with anti-miR-22-3p partially reversed the suppressive effects of catalpol treatment on the cell proliferative, cell invasive and migratory abilities of Huh7 and HCCLM3 cells (Fig. 4E-4L).

3.5. MiR-22-3p directly targeted MTA3 3′UTR

Due to the fact that miRNA targeted the 3′UTR of corresponding genes to regulate the gene expression levels, the bioinformatics analysis (online targetscan prediction tool) was further performed to determine

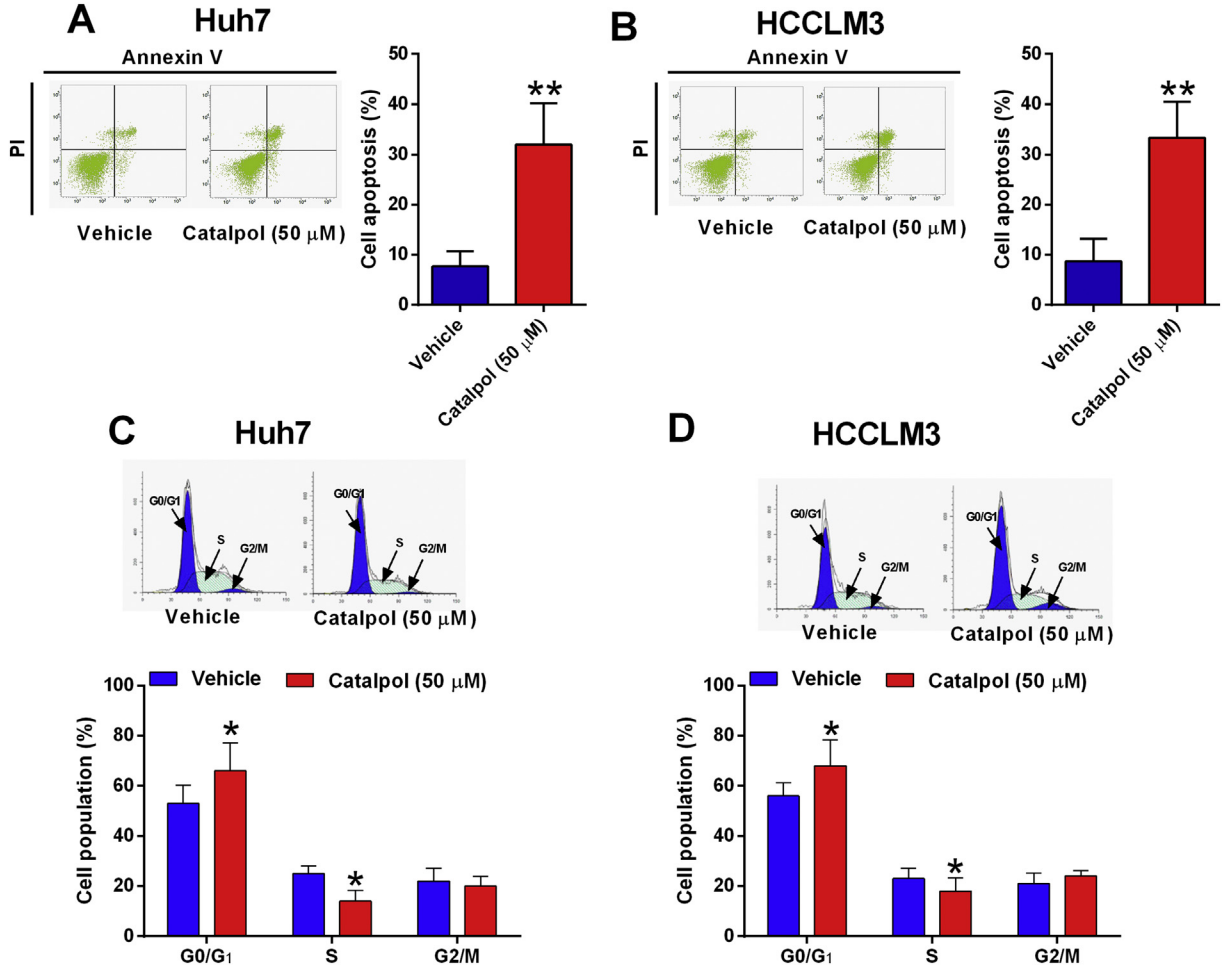

Fig. 3. Catalpol induced cell apoptosis and cell cycle arrest at G_0/G_1 phase of HCC cells. (A and B) The cell apoptosis of Huh7 and HCCLM3 was determined by flow cytometry. Cells were treated with vehicle or catalpol (50 μM) for 48 h. (C and D) The cell cycle of Huh7 and HCCLM3 was determined by flow cytometry. Cells were treated with vehicle or catalpol (50 μM) for 48 h. PI = propidium iodide. N = 3; *P < .05 and **P < .01 versus the vehicle group.

the potential targets of miR-22-3p, and among all the predicted targets of miR-22-3p, MTA3 was further selected for its documented role in cancer cell metastasis. In order to verify the physical interaction between MTA3 3′UTR and miR-22-3p, the reporter vectors containing either wild type MTA3 3′UTR or MTA3 3′UTR with point mutations were constructed (Fig. 5A). Treatment with miR-22-3p mimics markedly attenuated the luciferase activity of wild type vectors, but not the one of the mutant vectors in HCCLM3 cells (Fig. 5B and C). In addition, overexpression of miR-22-3p also significantly suppressed the mRNA and protein expression levels of MTA3 in HCCLM3 cells (Fig. 5D and E). Furthermore, overexpression of MTA3 was performed by transfecting HCCLM3 cells with pcDNA3.1-MTA3 (a constructed MTA3 overexpressing pcDNA3.1 vector; Fig. 5F and G), and MTA3 overexpression partly restored the suppressive actions of miR-22-3p overexpression on the MTA3 expression in HCCLM3 cells (Fig. 5H and I).

3.6. Catalpol inhibited cell proliferative, invasive and migratory of HCC cells via suppressing MTA3 expression

Catalpol (50 μM) with treatment for 48 h markedly down-regulated the MTA3 expression in HCCLM3 cells (Fig. 6A and B). To explore the mechanisms of MTA in mediating the tumor-suppressive actions of catalpol, we transfected the HCCLM3 cells with MTA3-overexpressing vector (pcDNA3.1-MTA3), and at 24 h after transfection, HCCLM3 cells received catalpol (50 μM) for 48 h treatment followed by different in vitro functional assays. As shown in Fig. 6C-6F, overexpression of MTA3 significantly increased the cell proliferative, cell invasive and migratory abilities of HCCLM3 cells, and the inhibitory actions of catalpol treatment on the cell viability, cell growth, cell invasion and migration of HCCLM3 were also partially reversed by MTA3 overexpression (Fig. 6C-6F).

3.7. Catalpol exerted inhibitory effects on the tumor growth in the xenograft mice model

The xenograft nude mice model was used to evaluate the in vivo anti-tumor potentials of catalpol, and the xenograft nude mice were treated with different doses of catalpol. The tumor volume was monitored every 5 days for 30 days, and as shown in Fig. 7A, catalpol treatment dose-dependently reduced the tumor volume (Fig. 7A). In addition, the weight of the dissected tumor was also significantly reduced in the catalpol groups when compared to vehicle group (Fig. 7B). Additionally, analysis of miR-22-3p and MTA mRNA expression levels in dissected tumor tissues showed that catalpol treatment also dose-dependently increased the miR-22-3p expression level (Fig. 7C), while decreased the MTA3 mRNA expression level (Fig. 7D).

4. Discussion

Due to the difficulties in early diagnosis and poor prognosis of HCC patients with advanced HCC, HCC continues to have an extremely high death rate and management of HCC is rather complex compared to

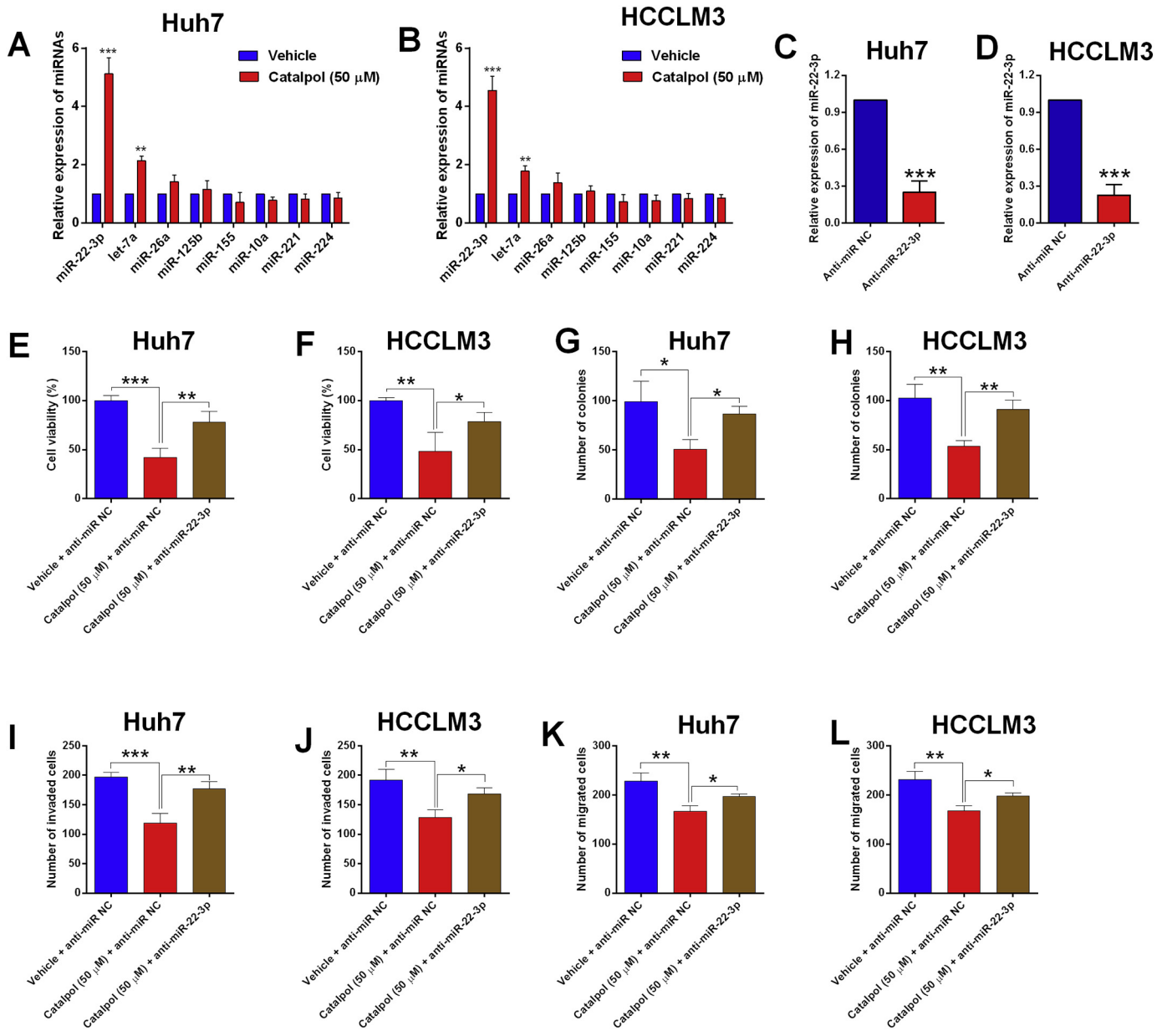

Fig. 4. Catalpol inhibited cell proliferation, invasion and migration of HCC cells via up-regulating miR-22-3p. (A and B) The expression levels of miRNAs in Huh7 and HCCLM3 cells were determined by qRT-PCR assay, cells were treated with vehicle or catalpol (50 μM) for 48 h. (C and D) The expression of miR-22-3p were determined by qRT-PCR assay in Huh7 and HCCLM3 cells at 24 h after transfection with anti-miR NC or anti-miR-22-3p. (E and F) The cell viability of Huh7 and HCCLM3 cells was determined by MTT assay. Cells were transfected with anti-miR NC or anti-miR-22-3p, and at 24 h after transfection, cells were treated with vehicle or catalpol (50 μM) for 48 h. (G-H) The cell growth of Huh7 and HCCLM3 cells was determined by colony formation assay. Cells were transfected with anti-miR NC or anti-miR-22-3p, and at 24 h after transfection. Cells were treated with vehicle or catalpol (50 μM) for 48 h. (I and J) The cell invasion of Huh7 and HCCLM3 cells measured by transwell cell invasion assay. Cells were transfected with anti-miR NC or anti-miR-22-3p, and at 24 h after transfection, cells were treated with vehicle or catalpol (50 μM) for 48 h. (K and L) The cell migration of Huh7 and HCCLM3 cells measured by transwell cell migration assay. Cells were transfected with anti-miR NC or anti-miR-22-3p, and at 24 h after transfection, cells were treated with vehicle or catalpol (50 μM) for 48 h. $N = 3$; $^{*}P < .05$, $^{**}P < .01$ and $^{***}P < .001$.

other malignancy. Recently, agents found in natural compounds have ben identified to possess anti-tumor potentials in HCC. In the current investigations, we evaluated the tumor-suppressive potentials of catalpol in HCC, and we found that catalpol concentration- and time-dependently suppressed the cell viability of HCC cells. Further functional assays showed that catalpol suppressed cell growth, cell invasive and migratory abilities, increased the rates of apoptotic cells and proportions of HCC cells at G_0/G_1 cell cycle phase. In addition, the mechanistic studies also showed that catalpol induced the up-regulation of miR-22-3p in HCC cells and the inhibitory effects of catalpol in HCC cell progression was mediated via miR-22-3p. Furthermore, miR-22-3p negatively regulated MTA3 expression in HCC cells, and miR-22-3p/MTA3 axis was demonstrated to involve in the anti-tumor actions of catalpol in HCC.

The anti-tumor mechanisms of catalpol have been implicated in several lines of studies in different types of cancers. Jin et al., demonstrated that catalpol suppressed cell proliferative ability of bladder cancer by increased cell apoptotic via inactivation of Akt-regulated anti-apoptotic pathway (Jin et al., 2015). Catalpol showed its anti-tumor effects in colorectal cancer via suppressing tumor angiogenesis and alleviating inflammation (Zhu et al., 2017). Wang et al., reported that catalpol suppressed cell proliferative ability via suppressing

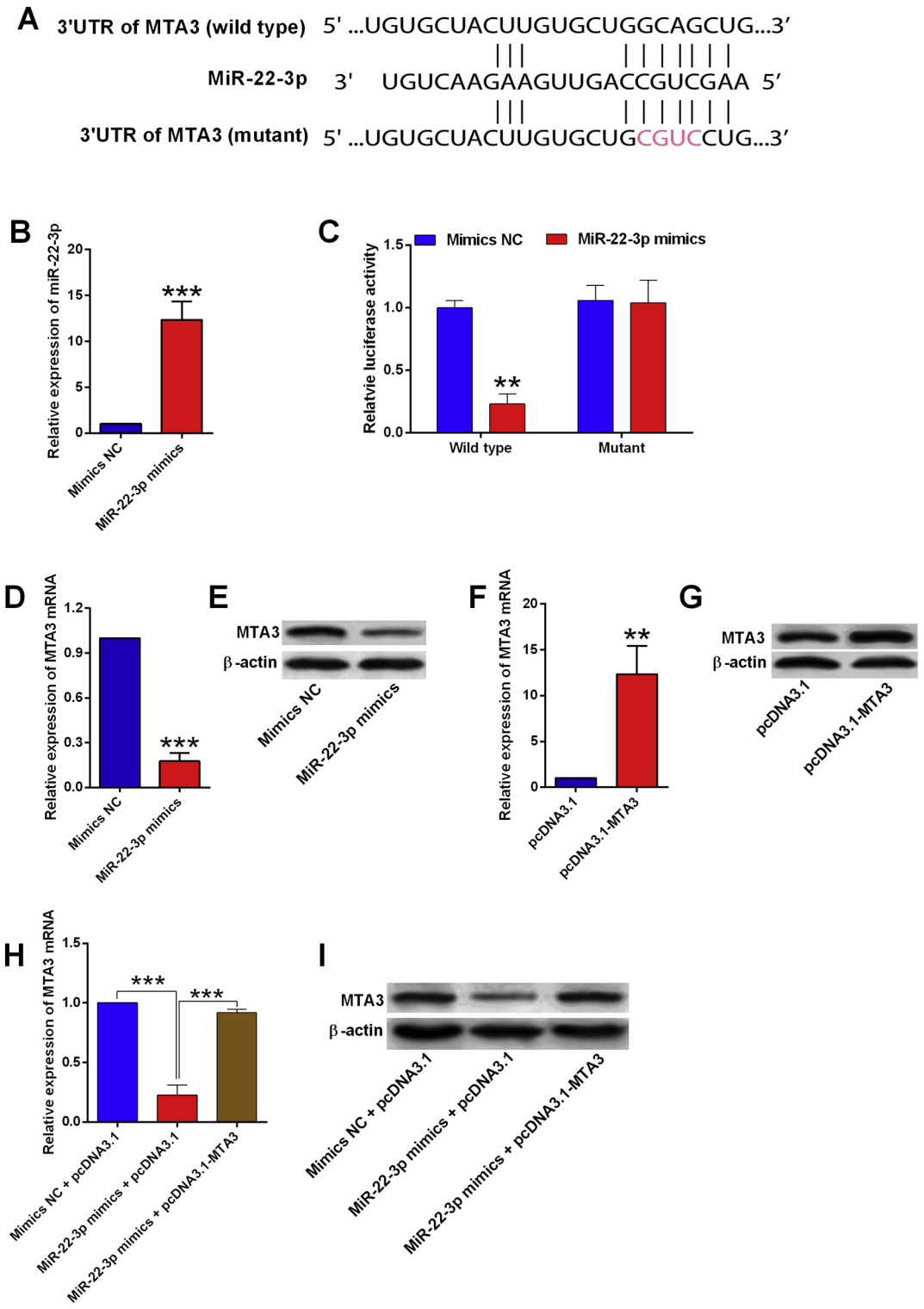

Fig. 5. MiR-22-3p directly targeted 3′UTR of MTA3. (A) The predicted binding sites between miR-22-3p and 3′UTR of MTA3; and pink nucleotides were the mutated sites. (B) HCCLM3 cells were transfected with mimics NC or miR-22-3p mimics, and at 24 h after transfection, the expression level of miR-22-3p was determined by qRT-PCR. (C) HCCLM3 cells were co-transfected with miRNAs oligos (mimics NC or miR-22-3p mimics) and luciferase reporter vectors (containing wild type or mutant 3′UTR of MTA3), and at 24 h after transfection, the luciferase activity was determined by the dual luciferase report system. (D and E) HCCLM3 cells were transfected with mimics NC or miR-22-3p mimics, and at 24 h after transfection, the mRNA and protein expression levels of MTA3 were determined by qRT-PCR and western blot, respectively. (F and G) HCCLM3 cells were transfected with pcDNA3.1 or pcDNA3.1-MTA3, and at 24 h after transfection, the mRNA and protein expression levels of MTA3 were determined by qRT-PCR and western blot, respectively. (H and I) HCCLM3 cells were co-transfected with mimics NC + pcDNA3.1, miR-22-3p mimics + pcDNA3.1 or miR-22-3p mimics + pcDNA3.1-MTA3, at 24 h after transfection, the mRNA and protein expression levels of MTA3 were determined by qRT-PCR and western blot, respectively. N = 3; **P < .05 and ***P < .001. (For interpretation of the references to colour in this figure legend, the reader is referred to the web version of this article.)

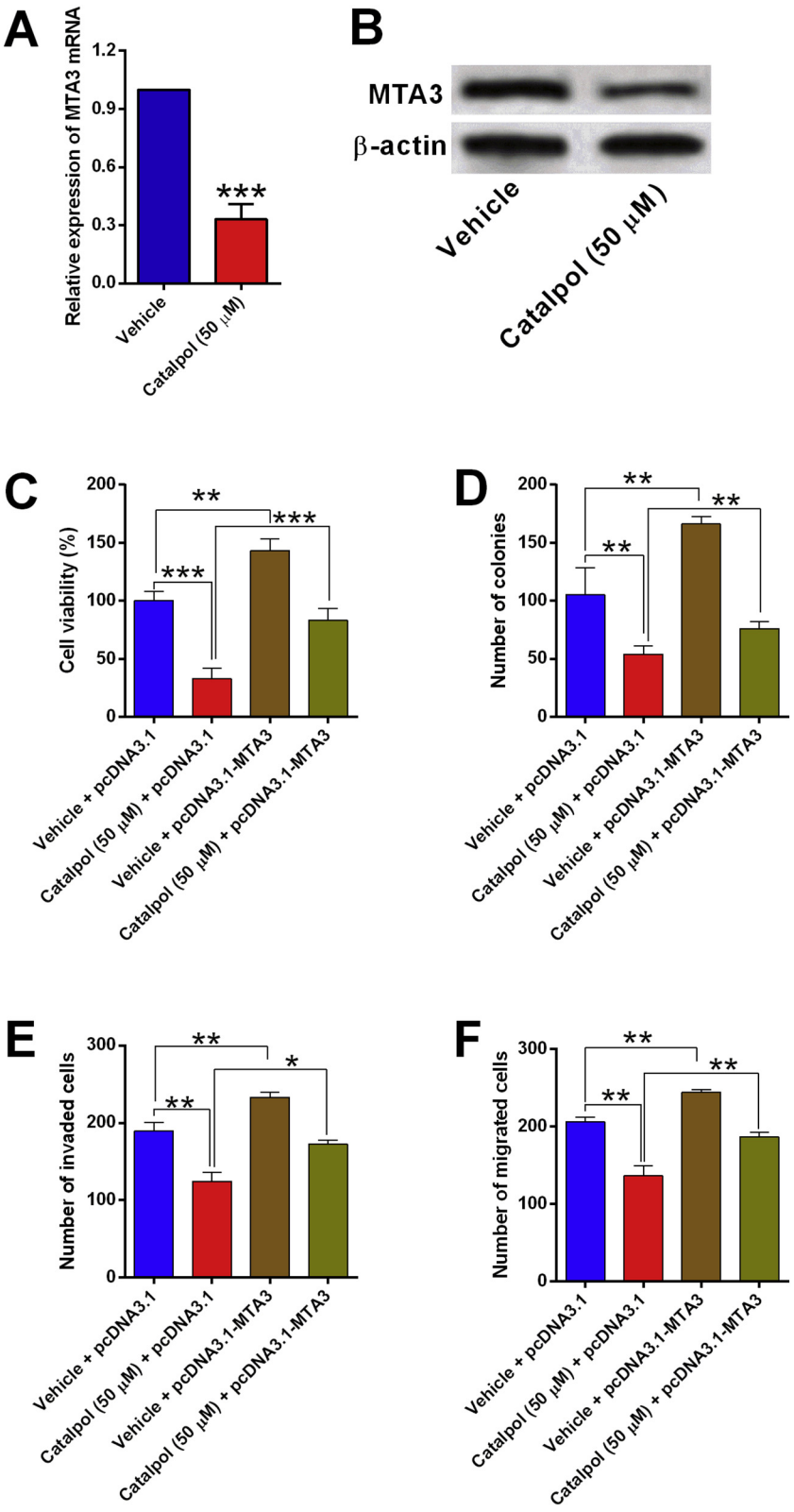

Fig. 6. Catalpol inhibited cell proliferation, invasion and migration of HCC cells via suppressing MTA3. (A and B) HCCLM3 cells were treated with vehicle or catalpol (50 μM) for 48 h, and the mRNA and protein expression levels of MTA3 were determined by qRT-PCR and western blot, respectively. (C–F) HCCLM3 cells were transfected with pcDNA3.1 or pcDNA3.1-MTA3, and at 24 h after transfection, HCCLM3 cells were treated with vehicle or catalpol (50 μM) for 48 h. (C) cell viability, (D) cell growth, (E) cell invasion and (F) cell migration were determined by MTT, colony formation, transwell invasion and migration assays, respectively. N = 3; *P < .05, **P < .01 and ***P < .001.

epithelial-mesenchymal transition (EMT) and promoting apoptosis in osteosarcoma (Wang and Xue, 2018). In the lung cancer studies, catalpol suppressed-induced EMT induced by TGF-β1 via suppressing Smad2/3 and NF-κB signalling (Li et al., 2018). Consistently, our experimental data revealed that catalpol treatment suppressed the suppressed cell growth, cell invasive and migratory abilities, increased the rates of apoptotic cells and proportions of HCC cells at G_0/G_1 cell cycle phase in the HCC cell lines. In addition, catalpol treatment also suppressed in vivo tumor growth of the xenograft mice. Taken together, these results indicated that catalpol exerted tumor-suppressive effects on the HCC cells.

To further explore the potential molecular mechanisms regarding the tumor-suppressive actions of catalpol in HCC. We assessed the effects of catalpol on the expression of the miRNAs that have been

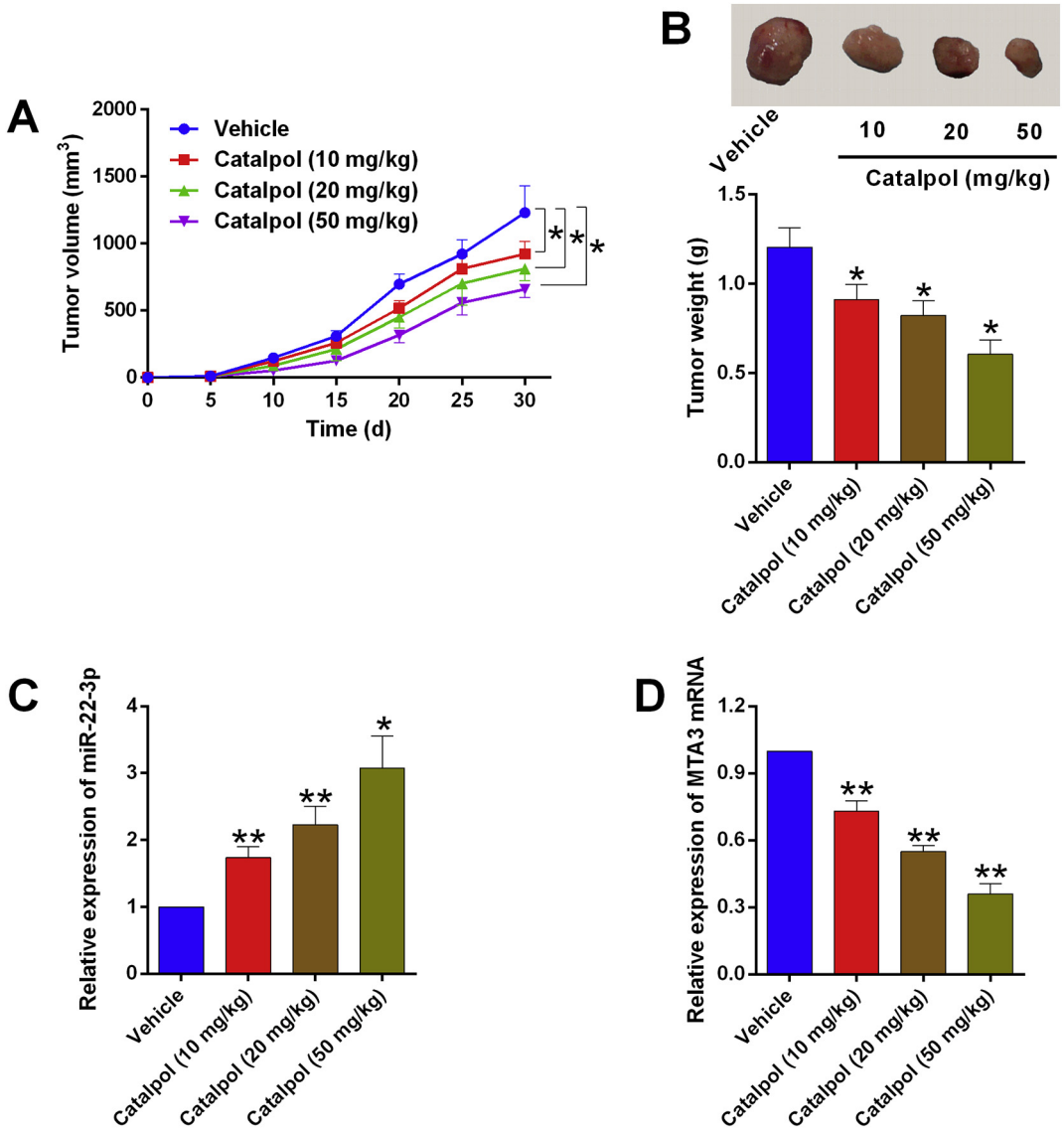

Fig. 7. Catalpol inhibited in vivo tumor growth in the xenograft mice model. (A) The tumor volume in the xenograft mice received different doses of catalpol treatment was determined very 5 days for 30 days. (B) The weight of the dissected tumors from the xenograft mice with different doses of catalpol treatments was determined. (C-D) The miR-22-3p expression and MTA mRNA expression in the dissected tumor tissues were determined by qRT-PCR assay. $N = 5$; *P < .05 and **P < .01 versus the vehicle group.

reported in regulating progression of HCC, and we identified miR-22-3p as the most regulated miRNA. In this regard, miR-22-3p was selected for further investigation. Based on the previous studies, miR-22-3p was identified to exert tumor-suppressive actions in various types of cancer including thyroid cancer, retinoblastoma, pancreatic cancer, HCC, cervical cancer and gastric cancer (Chen et al., 2016; Huang et al., 2018; Hussein et al., 2017; Liu et al., 2018; Lv et al., 2018; Wang et al., 2018a). As miR-22-3p suppressed HCC cell proliferative ability, the actions of catalpol treatment on HCC cell proliferative, cell invasive and migratory abilities under the condition of miR-22-3p knockdown were determined. MiR-22-3p knockdown attenuated the inhibitory effects of catalpol on HCC cell progression, suggesting that the tumor-suppressive effects of catalpol in HCC may be mediated via up-regulating miR-22-3p overexpression.

As miRNAs regulate gene expression via targeting the corresponding gene's 3′UTR, bioinformatics prediction was carried out to explore potential downstream targets of miR-22-3p. Among the predicted targets, MTA3 was further selected for investigation, as MTA3 has been demonstrated to promote cancer cell proliferation in various cancers such as clear-cell renal carcinoma (Ding et al., 2017), colorectal cancer (Jiao et al., 2017), breast cancer (Si et al., 2015) and lung cancer (Li et al., 2013). MTA3 is a member of the small protein family (Li et al., 2013). In the HCC, studies have shown that overexpression of MTA3 correlated with poor prognosis and advanced tumor progression in HCC (Wang et al., 2017), suggesting the oncogenic role of MTA3 in HCC. In our current investigations, we showed that MTA3 overexpression promoted cell proliferative, cell invasive and migratory abilities of HCC cells, and also attenuated the anti-tumor potentials of catalpol. All in all, these experimental results indicated that catalpol exerted its tumor-suppressive actions in HCC via repressing MTA3 expression.

5. Conclusions

In summary, our experimental data for the first time revealed the anti-tumor effects of catalpol in HCC, and the anti-tumor actions of catalpol were via regulating the miR-22-3p/MTA3 axis in HCC. These findings may imply that catalpol could represent a potential candidate to suppress human HCC progression.

Acknowledgement

This study was supported by National Standardization Project of Traditional Chinese Medicine-Standardization Construction of Radix Rehmanniae and Other Three Kinds of Traditional Chinese Medicine Pieces(ZYBZH-Y-HEN-18), National Key R&D Program: Key Special Projects of Modernization of Traditional Chinese Medicine-Research on Key Technologies of the Industry Chain of Radix Rehmanniae Characteristic Chinese Medicinal Materials (2017YFC1702800), and The Outstanding Youth Project of Scientific and Technological Innovation in Henan Province (No. 184100510017)

Conflict of interest

None.

References

Chen, J., et al., 2016. Berberine upregulates miR-22-3p to suppress hepatocellular carcinoma cell proliferation by targeting Sp1. Am. J. Transl. Res. 8, 4932–4941.
Clark, T., et al., 2015. Hepatocellular carcinoma: review of epidemiology, screening, imaging diagnosis, response assessment, and treatment. Curr. Probl. Diagn. Radiol. 44, 479–486.
Ding, D., et al., 2017. MiR-367 regulates cell proliferation and metastasis by targeting metastasis-associated protein 3 (MTA3) in clear-cell renal cell carcinoma. Oncotarget. 8, 63084–63095.
Forner, A., et al., 2012. Hepatocellular carcinoma. Lancet. 379, 1245–1255.
Gao, N., et al., 2014. Catalpol suppresses proliferation and facilitates apoptosis of OVCAR-3 ovarian cancer cells through upregulating microRNA-200 and downregulating MMP-2 expression. Int. J. Mol. Sci. 15, 19394–19405.
Grandhi, M.S., et al., 2016. Hepatocellular carcinoma: from diagnosis to treatment. Surg. Oncol. 25, 74–85.
Huang, Y., et al., 2018. Serum microRNA panel excavated by machine learning as a potential biomarker for the detection of gastric cancer. Oncol. Rep. 39, 1338–1346.
Hussein, N.A., et al., 2017. Plasma miR-22-3p, miR-642b-3p and miR-885-5p as diagnostic biomarkers for pancreatic cancer. J. Cancer Res. Clin. Oncol. 143, 83–93.
Jiao, T., et al., 2017. MTA3 regulates malignant progression of colorectal cancer through Wnt signaling pathway. Tumour Biol. 39, 1010428317695027.
Jin, D., et al., 2015. Catalpol inhibited the proliferation of T24 human bladder cancer cells by inducing apoptosis through the blockade of Akt-mediated anti-apoptotic signaling. Cell Biochem. Biophys. 71, 1349–1356.
Khemlina, G., et al., 2017. The biology of hepatocellular carcinoma: implications for genomic and immune therapies. Mol. Cancer 16, 149.
Li, H., et al., 2013. Overexpression of MTA3 correlates with tumor progression in non-small cell lung cancer. PLoS One 8, e66679.
Li, X., et al., 2014. Hypoglycemic effect of catalpol on high-fat diet/streptozotocin-induced diabetic mice by increasing skeletal muscle mitochondrial biogenesis. Acta Biochim. Biophys. Sin. Shanghai 46, 738–748.
Li, Z., et al., 2018. Tumor-secreted Exosomal miR-222 promotes tumor progression via regulating P27 expression and re-localization in pancreatic Cancer. Cell. Physiol. Biochem. 51, 610–629.
Liu, C., et al., 2015. Catalpol suppresses proliferation and facilitates apoptosis of MCF-7 breast cancer cells through upregulating microRNA-146a and downregulating matrix metalloproteinase-16 expression. Mol. Med. Rep. 12, 7609–7614.
Liu, L., et al., 2017. Catalpol promotes cellular apoptosis in human HCT116 colorectal cancer cells via microRNA-200 and the downregulation of PI3K-Akt signaling pathway. Oncol. Lett. 14, 3741–3747.
Liu, Y., et al., 2018. MiR-22-3p targeting alpha-enolase 1 regulates the proliferation of retinoblastoma cells. Biomed. Pharmacother. 105, 805–812.
Lv, K.T., et al., 2018. MiR-22-3p regulates cell proliferation and inhibits cell apoptosis through targeting the eIF4EBP3 gene in human cervical squamous carcinoma cells. Int. J. Med. Sci. 15, 142–152.
Morishita, A., Masaki, T., 2015. miRNA in hepatocellular carcinoma. Hepatol. Res. 45, 128–141.
Ozer Etik, D., et al., 2017. Management of Hepatocellular Carcinoma: prevention, surveillance, diagnosis. and Staging. Exp Clin Transplant. 15, 31–35.
Si, W., et al., 2015. Dysfunction of the reciprocal feedback loop between GATA3- and ZEB2-nucleated repression programs contributes to breast Cancer metastasis. Cancer Cell 27, 822–836.
Wang, L., Xue, G.B., 2018. Catalpol suppresses osteosarcoma cell proliferation through blocking epithelial-mesenchymal transition (EMT) and inducing apoptosis. Biochem. Biophys. Res. Commun. 495, 27–34.
Wang, Z.H., Zhan-Sheng, H., 2018. Catalpol inhibits migration and induces apoptosis in gastric cancer cells and in athymic nude mice. Biomed. Pharmacother. 103, 1708–1719.
Wang, C., et al., 2017. Overexpression of the metastasis-associated gene MTA3 correlates with tumor progression and poor prognosis in hepatocellular carcinoma. J. Gastroenterol. Hepatol. 32, 1525–1529.
Wang, M., et al., 2018a. CircRNA circ-ITCH suppresses papillary thyroid cancer progression through miR-22-3p/CBL/beta-catenin pathway. Biochem. Biophys. Res. Commun. 504, 283–288.
Wang, Z., et al., 2018b. Catalpol inhibits TGF-beta1-induced epithelial-mesenchymal transition in human non-small-cell lung cancer cells through the inactivation of Smad2/3 and NF-kappaB signaling pathways. J. Cell. Biochem. 120, 2251–2258.
Xu, X., et al., 2018. The role of MicroRNAs in hepatocellular carcinoma. J. Cancer 9, 3557–3569.
Zheng, X.W., et al., 2017. Neuroprotection of Catalpol for experimental acute focal ischemic stroke: preclinical evidence and possible mechanisms of Antioxidation, anti-inflammation, and Antiapoptosis. Oxidative Med. Cell. Longev. 2017, 5058609.
Zhu, P., et al., 2017. Catalpol suppressed proliferation, growth and invasion of CT26 colon cancer by inhibiting inflammation and tumor angiogenesis. Biomed. Pharmacother. 95, 68–76.